Construction of Smart Supramolecular Polymeric Hydrogels Cross-linked by Discrete Organoplatinum(II) Metallacycles via Post-Assembly Polymerization

Wei Zheng,[†] Li-Jun Chen,[†] Guang Yang,[‡] Bin Sun,[†,‖] Xu Wang,[‖] Bo Jiang,[†] Guang-Qiang Yin,[†] Li Zhang,[§] Xiaopeng Li,[‖] Minghua Liu,[§] Guosong Chen,*[,‡] and Hai-Bo Yang*[,†]

[†]Shanghai Key Laboratory of Green Chemistry and Chemical Processes, School of Chemistry and Molecular Engineering, East China Normal University, Shanghai 200062, People's Republic of China

[‡]The State Key Laboratory of Molecular Engineering of Polymers and Department of Macromolecular Science, Fudan University, Shanghai 200433, People's Republic of China

[§]Key Laboratory of Colloid, Interface and Chemical Thermodynamics, Institute of Chemistry, The Chinese Academy of Sciences, Beijing 100080, People's Republic of China

[‖]Department of Chemistry and Biochemistry & Materials Science, Engineering, and Commercialization Program, Texas State University, San Marcos, Texas 78666, United States

S *Supporting Information*

ABSTRACT: Postassembly modification strategy has been successfully employed in the construction of discrete metallosupramolecular assemblies. However, the most known reports have been limited to the simple structural conversion through the easy covalent reactions, thus hindering the development of organometallic functional materials. In this study, we first combined coordination-driven self-assembly and postassembly reversible addition–fragmentation chain-transfer (RAFT) polymerization to produce a new family of star supramolecular polymers containing well-defined metallacycles as cores, which featured typical lower critical solution temperature (LCST) behavior in water because of the existence of poly(N-isopropylacrylamide) (PNIPAAM) moieties. Moreover, the obtained star polymers could further form supramolecular hydrogels cross-linked by discrete hexagonal metallacycles at room temperature without heating–cooling process. Interestingly, the resultant polymeric hydrogels exhibited stimuli-responsive behavior toward temperature and bromide anion as well as self-healing property. We demonstrated that the dynamic nature of Pt–N bonds in the hexagonal metallacycles played an important role in determining the stimuli-responsive and self-healing property of the final soft matters. Thus, merging coordination-driven self-assembly and postassembly polymerization provided a new avenue to the preparation of functional materials containing well-defined, discrete metal–organic assemblies as main scaffolds.
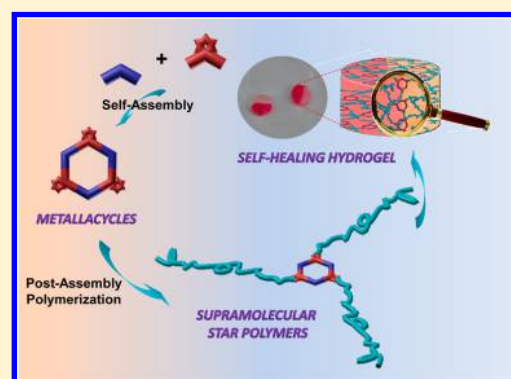
INTRODUCTION

During the past few decades, coordination-driven self-assembly has evolved to be a highly efficient strategy for producing discrete two-dimensional (2-D) polygons and three-dimensional (3-D) polyhedra with well-defined shapes and sizes.[1,2] These metallosupramolecular architectures are of particular interest not only for their aesthetic attributes but also because of their broad applications in fields such as catalysis, sensors, and supramolecular devices, etc.[3] With the aim to develop novel organometallic materials with the desired functionalities and applications, recent research effort has been devoted to the functionalization of discrete metallosupramolecular structures.[4] Although the construction of functionalized metallacycles or metallacages could be realized by employing prefunctionalized moieties via coordination-driven self-assembly,[5] the library and

scope of possible building blocks sometimes suffers from the potential incompatibilities and interferences of the functionalities with the assembly process. Thus, the development of a highly efficient strategy for functionalization of discrete metallosupramolecular architectures is still in great demand.

Postassembly modification strategy has been widely employed to tune the structures and functionalities of biological scaffolds in nature.[6] Inspired by a great number of successful examples on postassembly modification in biological systems, postassembly modification of supramolecular architectures has been extensively explored in the fields of metal–organic frameworks (MOFs),[7] mechanically interlocked systems,[8]

Scheme 1. Graphical Representation of Synthesis of Organoplatinum(II) Metallacycles and Star Supramolecular Polymers
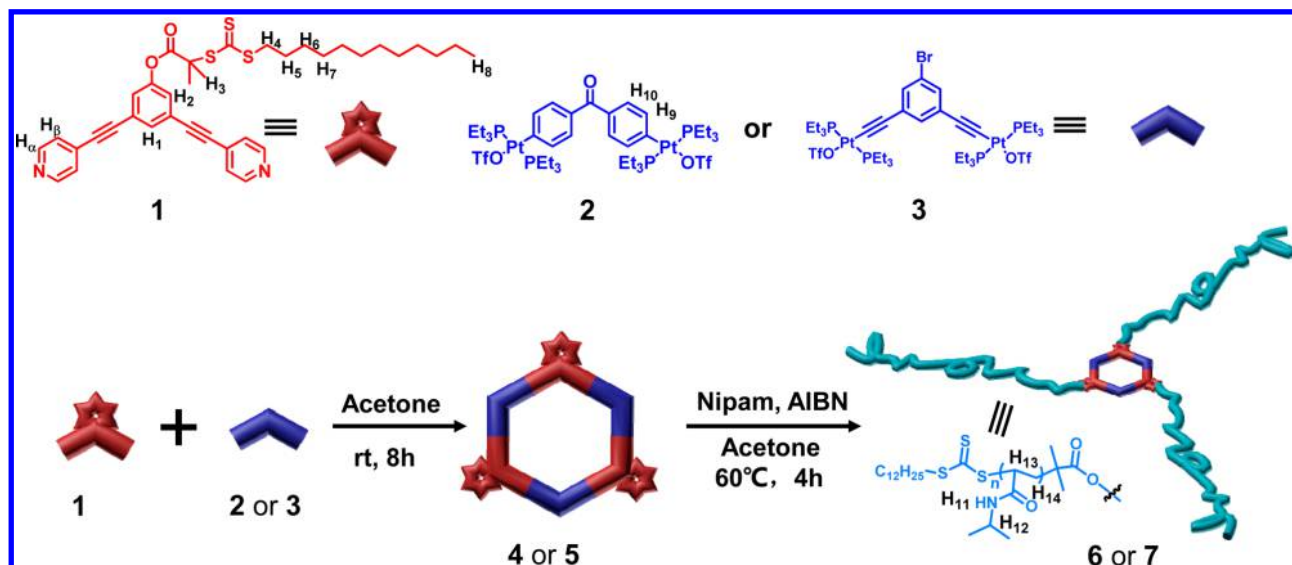
covalently modifying polymer,[9] etc. This strategy allows for fine-tuning the structure of supramolecular species, thus leading to the higher order complexity and additional functionality after the initial self-assembly. During the past years, functionalization of discrete metallosupramolecular complexes has been investigated by employing postassembly modification strategy.[10] In general, postassembly modification of discrete metallacycles or metallacages can be obtained through simple covalent reaction or supramolecular transformation. For example, Stang and co-workers have reported postassembly functionalization of discrete organometallic assemblies via simple organic reactions such as copper-free click chemistry and Diels−Alder reactions, respectively.[11] In addition, Nitschke and co-workers successfully realized multistep transformation of metallo-organic structures by employing imine exchange guided by the Hammett equation.[12] Moreover, we prepared a new family of multibisthienylthene hexagons with multiple photochromic units via coordination-driven self-assembly, which were found to undergo the quantitative reversible supramolecular transformation triggered by light irradiation.[13] Thus, postassembly modification has proven to be a highly efficient strategy to realize functionalization of discrete metallosupramolecular structures with fine-tuning structures and desired properties.

Although postassembly modification has been successfully employed in the construction of novel discrete metallosupramolecular assemblies, the most known reports have been still limited to the simple structural conversion through the easy covalent reactions. Thus, it is deeply expected to realize postassembly modification of discrete organometallic architectures with specific outputs such as tailored properties or functions. Over the past decades, controlled radical polymerization (CRP) has been extensively explored in the preparation of functional polymers,[14−17] which has provided a convenient route for producing polymeric materials with well-controlled structures and desired functions. Stimulated by numerous successful examples of functional polymeric macromolecules, we envisioned that merging coordination-driven self-assembly and controlled radical polymerization, that is, postassembly polymerization, would pave a new avenue to the preparation of well-defined functional polymers based on discrete metallosupramolecular scaffold. As compared to the most previous

study on postassembly modification of discrete metallacycles or metallacages by employing simple organic reaction, postassembly polymerization not only allows for the construction of the higher-order complex architectures but also provides more opportunities in the preparation of new functional materials because of the existence of a wide range of polymerization reactions.

Herein, we present the successful combination of coordination-driven self-assembly and postassembly reversible addition−fragmentation chain-transfer (RAFT) polymerization to produce a new family of star supramolecular polymer containing well-defined metallacycles as cores. Surprisingly, the obtained star polymers could further form supramolecular polymeric hydrogels cross-linked by organoplatinum(II) metallacycles at room temperature without heating−cooling process. Further investigation revealed that the polymeric hydrogels exhibited both thermoresponsive property and bromide-induced stimuli-responsive behavior. More importantly, in virtue of the dynamic nature of supramolecular metallacycle, the obtained polymeric hydrogels displayed interesting self-healing property. Therefore, we report the first example of supramolecular polymeric hydrogel cross-linked by well-defined metallacycles through postassembly polymerization, thus providing a new route for producing novel functional materials containing discrete metallosupramolecular architectures.

■ RESULTS AND DISCUSSION

Construction of Discrete Hexagonal Metallacycles Decorated with Multiple CTAs Moieties via Coordination-Driven Self-Assembly. On the basis of the general principle of coordination-driven self-assembly, the size and shape of the final discrete metallacycles are mainly determined by the angle and symmetry of the selected building blocks.[1a] The formation of a discrete hexagonal metallacycle can be realized through the combination of three 120° donor building blocks and three 120° acceptor subunits.[18] In this study, a new 120° dipyridyl donor 1 containing chain transfer agents (CTAs) (Scheme S1) and 120° di-Pt(II) acceptors 2 and 3 were selected for the construction of discrete hexagonal metallacycles decorated with three CTAs moieties at the alternative vertexes. Multinuclear NMR (¹H and ³¹P) analysis
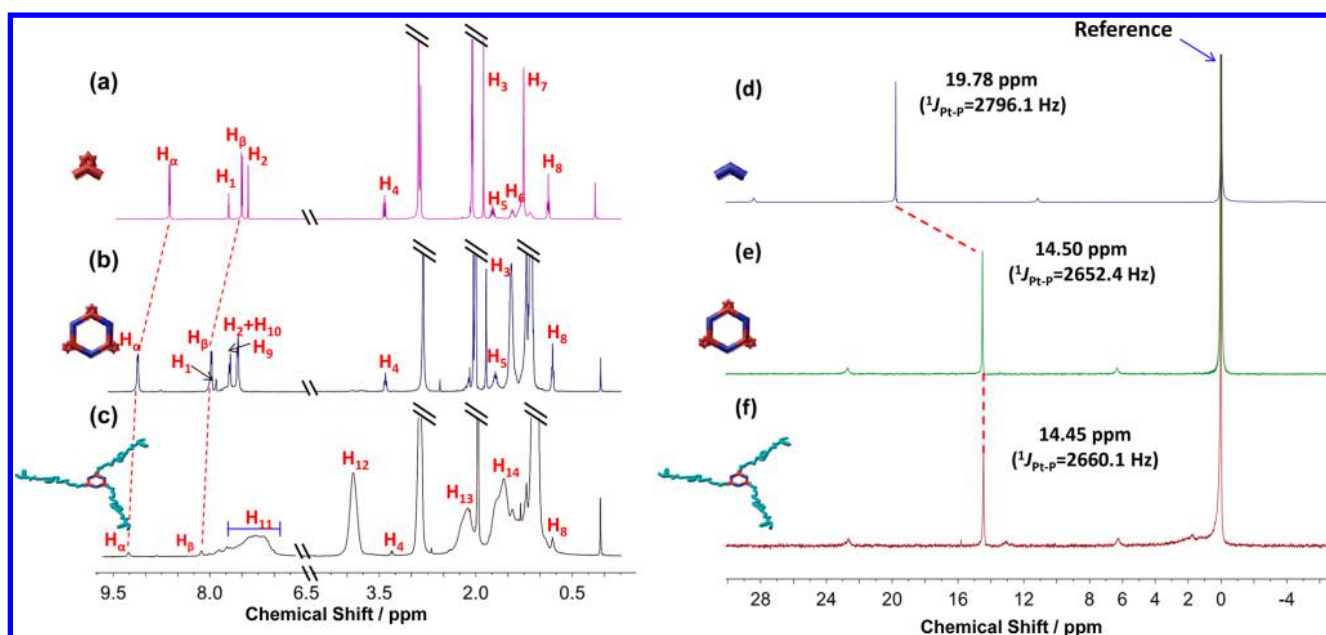
Figure 1. Partial ^{1}H NMR spectra (400 MHz, 298 K) of 120° dipyridyl donor **1** (a), hexagonal metallacycles **4** (b), and star supramolecular polymer **6** (c) in acetone-d_6. ^{31}P {^{1}H} NMR spectra (161.9 MHz, 298 K) of 120° di-Pt (II) acceptors **2** (d), hexagonal metallacycles **4** (e), and star supramolecular polymer **6** (f) in acetone-d_6.

of the reaction mixtures indicated the formation of discrete metallacycles with highly symmetric hexagonal scaffold (Scheme 1). The ^{31}P {^{1}H} NMR spectrum of hexagonal metallacycle **4**, for example, displayed a sharp singlet at 14.50 ppm shifted upfield from the starting platinum acceptor **2** by approximately 5.28 ppm. In addition, the protons of the pyridine rings exhibited obvious downfield shifts (α-H$_{Py}$, 0.46 ppm; β-H$_{Py}$, 0.45 ppm) caused by the loss of electron density upon coordination of the pyridine-N atom with the Pt(II) metal center (Figure 1). The formation of oligomers can be ruled out by the sharp NMR signals in both ^{31}P and ^{1}H NMR spectra along with the solubility of these assemblies. Electrospray ionization mass spectrometry (ESI-TOF-MS) technique has been recognized as an effective tool to determine the molecular composition of discrete metallosupramolecular architectures because it is able to keep the assembly intact to the maximum extent during the ionization process. Thus, ESI-TOF mass spectrometry was employed to provide further evidence for the formation of new hexagonal metallacycles. For example, in the mass spectrum of **4**, peaks at m/z = 1337.84 and m/z = 1040.60, corresponding to $[M - 4OTf]^{4+}$ and $[M - 5OTf]^{5+}$, respectively, were observed, and their isotopic resolutions are in excellent agreement with the theoretical distributions (Figure S1a). A similar mass result was obtained for metallacycle **5** (Figure S1b), which allowed for the molecularity of tris- CTAs hexagonal metallacycle to be unambiguously established.

Preparation and Characterization of Star Supramolecular Polymers. With the newly designed tris-CTAs metallacycles **4** and **5** in hand, the subsequent polymerization was carried out as shown in Scheme 1 (also see Schemes S3 and S5). With the aim to obtain the functional star supramolecular polymers, N-isopropylacrylamide (NIPAAM) was selected as monomer because PNIPAAM always displayed interesting thermoresponsive property such as LCST. Both star supramolecular polymers **6** and **7** were prepared by polymerizing NIPAAM in the presence of the corresponding tris-CTAs

metallacycles **4** or **5** and 2′,2-azobis(isobutyronitrile) (AIBN) as initiator with a molar ratio of [monomer]:[tris-CTAs metallacycle]:[AIBN] = 600:1:0.5 in acetone. After the mixture was degassed by three freeze−evacuate−thaw circles, the tube was sealed under vacuum. The subsequent polymerization was carried out at 60 °C for 4 h. Polymers **6** and **7** were isolated by precipitation in diethyl ether, collected by filtration, and dried in vacuum.

The typical absorption bands of PNIPAAM ($\nu_{C=O}$ = 1650 cm^{-1}) and (ν_{C-C} = 2971 cm^{-1}) were found in the FTIR spectra of polymers **6** and **7** (Figures S30 and S32) that provided strong support for the formation of star supramolecular polymers. The chemical structures of the obtained polymers were further characterized by multinuclear NMR (^{1}H and ^{31}P) spectroscopy. For example, the characteristic signals of PNIPAAM, including δ = 4.0 ppm and δ = 1.0 ppm attributed to the methine protons and methyl protons of isopropyl groups, respectively, δ = 6.5−7.5 ppm ascribed to the NH of amide groups, etc., were clearly observed in both ^{1}H NMR spectra of polymers **6** and **7**. Note that, as compared to the original tris-CTAs metallacycles **4** and **5**, the signals corresponding to pyridyl moieties remained almost unchanged, which indicated that the controlled RAFT polymerization did not destroy the metallacyclic scaffold. Moreover, the ^{31}P {^{1}H} NMR spectra of polymers **6** and **7** displayed a singlet at 14.45 and 16.31 ppm, respectively, which were consistent with that of the original tris-CTAs metallacycles (Figures 1 and S24). This finding again proved the maintenance of the hexagonal metallacycles in the obtained star supramolecular polymers.

The molecular weights of polymers **6** and **7** were determined to be $M_{n,NMR}$ = 52 000 g/mol and $M_{n,NMR}$ = 63 000 g/mol, respectively, obtained by ^{1}H NMR spectroscopic end-group analysis. In addition, gel permeation chromatography (GPC) analysis of polymers **6** and **7** revealed the number-averaged molecular weight ($M_{n,GPC}$) values to be 43 000 and 57 000 g/mol (Figure S2), respectively, with a relatively narrow molecular distribution (for polymer **6**, PDI = 1.25; for polymer
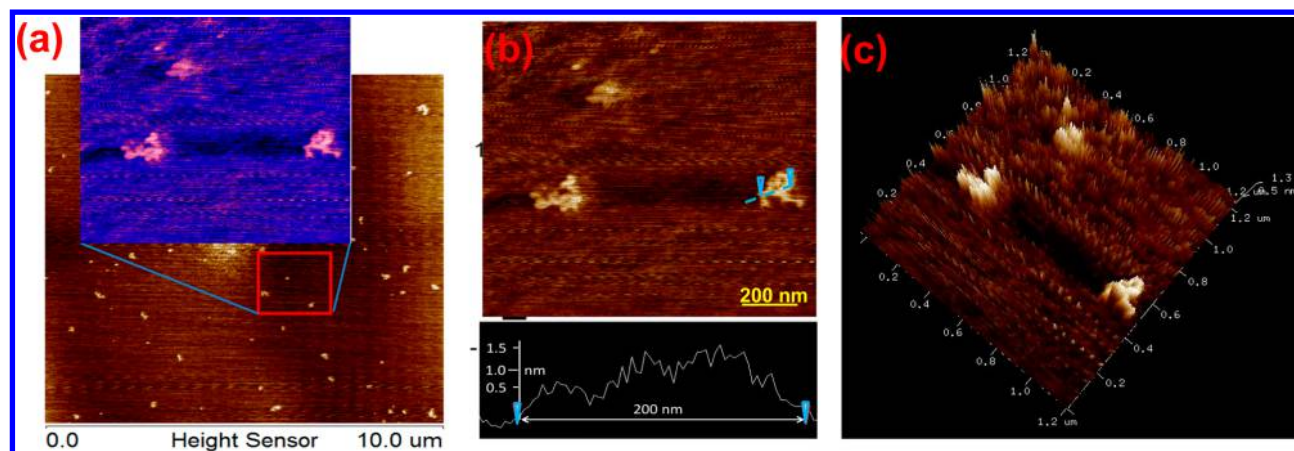
Figure 2. (a) General view of topographic AFM images of star supramolecular polymer **7**, (b) magnified objects showing the presence in their structure of internal bright spots, and (c) three-dimensional image.
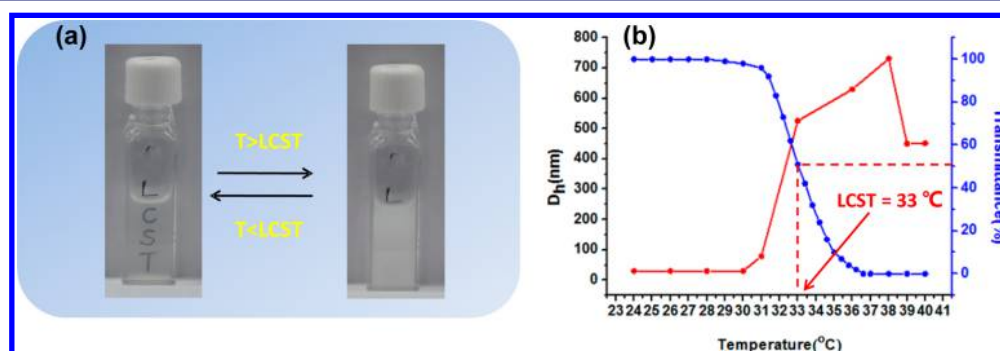

Figure 3. (a) Photograph showing an aqueous solution of star supramolecular polymer **6** (3.0 mg/mL) at room temperature (left) and at 35 °C (right), and (b) transmittance (blue line) and hydrodynamic diameter (red line) versus temperature for **6** (3.0 mg/mL) in aqueous solution.

7, PDI = 1.28). It should be noted that the GPC investigation of original tris-CTAs metallacycles **4** and **5** under the same condition was performed as well. The molecular weight of each metallacycle was found to be around 630, which was much smaller than that of the star polymers. Thus, the GPC investigation indicated that the RAFT polymerization of NIPAAM by employing tris-CTAs metallacycles as RAFT agents allowed for the formation of novel star supramolecular polymers. In addition, to obtain further evidence for the existence of star supramolecular polymers, AFM investigation was further carried out to visualize the obtained star supramolecular polymers. Because of the strong aggregation tendency of PNIPAAM, it was extremely difficult to obtain the AFM image of discrete star polymer. Thus, the AFM measurement of polymer **7** in very dilute solution (1×10^{-5} mg/mL) was performed. With considerable efforts, the star-shaped topology for polymer **7** was found in the AFM image (Figure 2), and the average height was found to be 1.0 nm. Moreover, this particular topology was highlighted in three-dimensional (3-D) images as shown in Figure 2c.

Thermoresponsive Behavior of the Obtained Star Supramolecular Polymers. PNIPAAM has evolved to be a widely investigated smart polymer that usually exhibits a LCST of ~32 °C.[19] Because of the existence of PNIPAAM moieties in the obtained star supramolecular polymers, the investigation of thermoresponsive behavior of polymers **6** and **7** was then carried out. Usually the organoplatinum metallacycles feature better solubility in common organic solvents than that in water. In this study, however, with the introduction of water-soluble

PNIPAAM groups, the resultant star polymers **6** and **7** became soluble in water. The primary study revealed that both polymers **6** and **7** displayed a LCST behavior. For example, the aqueous polymer solution of **6** was transparent and colorless at room temperature (Figure 3a). However, with the increase of temperature from 24 to 40 °C, the aqueous solution gradually turned into a white opaque suspension, and the polymers finally precipitated from water. Upon being cooled to room temperature, the transparent colorless solution was recovered. A similar phenomenon was observed in the case of polymer **7**. To determine the clouding point (T_{cloud}) of the obtained star polymers **6** and **7**, the investigation of the change in transmittance at 500 nm was carried out by employing a temperature-controlled UV/vis spectrometer. The experiment was conducted in aqueous solutions with a constant concentration of 3.0 mg/mL and a heating rate of 0.2 °C/min. As shown in Figure 3b and Figure S5, both polymers **6** and **7** displayed dramatic changes of transmittance around T_{cloud}, inferring a highly sensitive phase separation. The final T_{cloud} was determined to be 33 and 32 °C for polymers **6** and **7**, respectively, which was similar to the T_{cloud} value of the typical PNIPAAM. This finding indicated that the postassembly polymerization of discrete metallacycles with NIPAAM moiety allowed for the maintenance of LCST property of PNIPAAM. In addition, the dynamic light scattering (DLS) and variable-temperature (VT) ^{1}H NMR experiments in D_2O were performed to investigate the thermoresponsive behavior of star polymers **6** and **7**. It should be noted that the critical temperature of the phase transition obtained from both DLS

investigation (Figures 3b and S5) and ^{1}H NMR experiment (Figure S6) agreed with the result of transmittance measurements.

The thermoresponsive behavior of star supramolecular polymers **6** and **7** in aqueous solution (1 mg/mL) was further evaluated by using transmission electron microscopy (TEM), which provided visible evidence for the LCST transition process of these resultant polymers. As shown in Figure 4, for
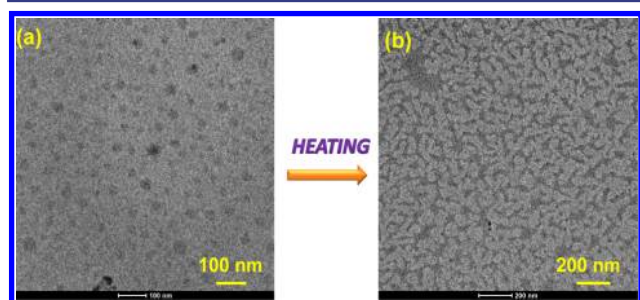

Figure 4. TEM images of star supramolecular polymer **6** (1 mg/mL) at 25 °C (a) and at 40 °C (b).

instance, in the case of polymer **6**, all aggregates were nearly spherical in shape with the average diameter of 20 nm at room temperature. Upon increasing the temperature to 40 °C, the multimicelle aggregates with the large size (~100 nm) were observed in the TEM images.

Supramolecular Polymeric Hydrogels Cross-linked by Organoplatinum(II) Metallacycles. The gel formation of NIPAAM polymerized metallacycles **6** and **7** in aqueous solutions was investigated by the "stable-to-inversion-of-test-tube" method. It was found that the aqueous solutions of **6** and **7** could form free-standing macroscopic hydrogels under room temperature only in 5 min (Figure 5). The critical gelator
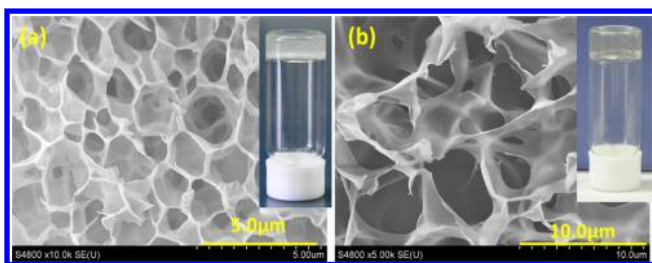

Figure 5. Photographs of polymeric hydrogel formation and SEM images of the xerogel: (a) star supramolecular polymer **6** and (b) star supramolecular polymer **7**.

concentrations (CGCs) were determined to be 2.5 wt % for **6** and 4.0 wt % for **7**, respectively. Notably, PNIPAAM containing dipyridine **8** derived from ligand **1** through RAFT polymerization (Scheme S6) was not able to form free-standing gel even with the higher concentration (>10.0 wt %). This control experiment indicated that the metallacyclic scaffold might play an important role of preorganization during the gelation process. The microstructures of these supramolecular hydrogels **6** and **7** were further investigated by using scanning electron micrography (SEM) after cryo-drying, which revealed very uniform, highly ordered porous cross-linked networks. The pore size of **6** was found to be approximately 2.0 μm, while the pore size of **7** was about 5.0 μm (Figure 5).

Mechanical strength and elasticity are important features of gel materials.[20] The rheological investigation can disclose the amount of energy stored in the gel system and energy dissipated within the system indicated by modulus (G') and the loss modulus (G''). Thus, investigation of the rheological properties of the obtained polymeric hydrogels was carried out. A frequency sweep from 50 to 0.1 rad/s was performed on each gel at small oscillatory stress of 1.0 Pa at 20 °C. Taking polymeric hydrogel of **6** (3.0 and 8.0 wt % concentration, respectively) as an example, the frequency dependence of the storage and loss oscillatory shear moduli (G' and G'', respectively) clearly identified the hydrogel-like behavior for star polymer **6** because the G' and G'' curves were linear and parallel with G' being dominant across the whole range of frequencies studied (Figure 6a). In addition, the elastic
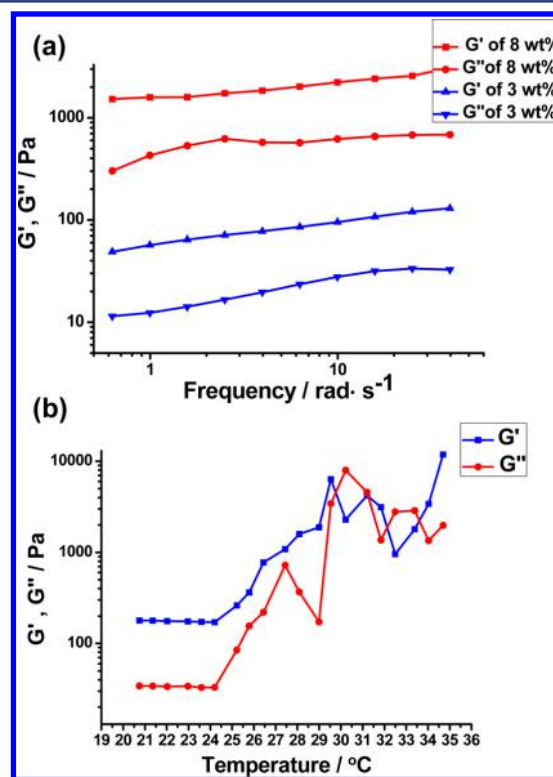

Figure 6. Rheological data of the polymeric hydrogels. (a) Frequency sweep results for the hydrogel of star supramolecular polymer **6**. (b) Temperature dependence of dynamic shear moduli (σ = 1 Pa, ω = 1 rad/s) for a 3.0 wt % hydrogel of star supramolecular polymer **6**.

modulus G' of the 3.0 wt % hydrogel was about 100 Pa, while the 8.0 wt % hydrogel was about 1200 Pa. Moreover, the 3.0 wt % hydrogel showed significantly lower values of G' and G'' than those of the 8.0 wt % hydrogel. According to Hvidt's classification,[21] the 3.0 wt % hydrogel could be considered a "soft gel" (i.e., G' < 1000 Pa), while the 8.0 wt % hydrogel could be considered "hard gels" (i.e., G' > 1000 Pa). The increase of the moduli upon increasing concentration indicated a strongly correlated behavior and suggested a self-similar behavior in the sense of a large-scale organization.

Stimuli-Responsive Behavior of the Obtained Polymeric Hydrogels. Interestingly, further investigation revealed that such obtained polymer hydrogels featured a volume phase-transition in response to the change in environmental temperature (Figure 7a and b). Below the LCST, the hydrogel
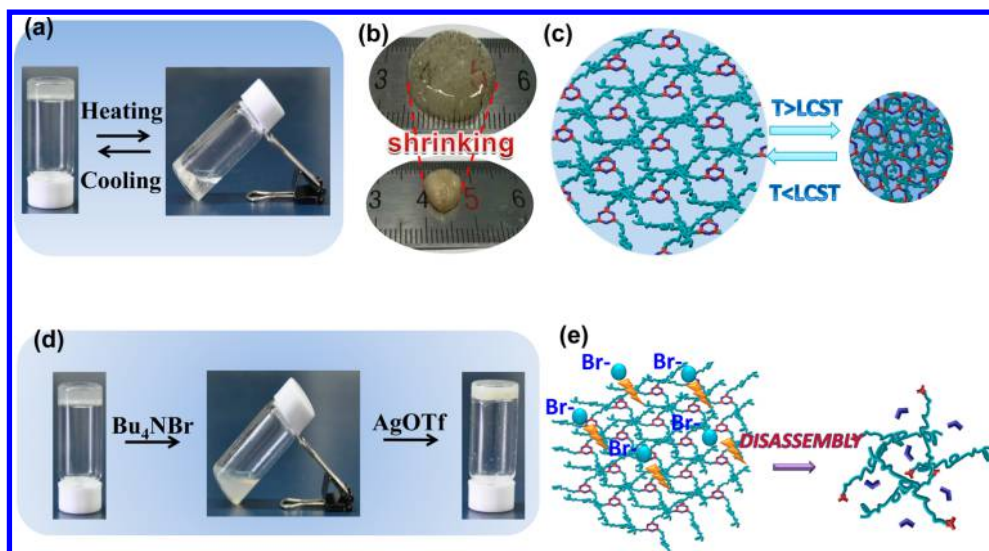
Figure 7. Thermosensitive property of the supramolecular polymeric hydrogel. (a) Reversible gel−sol transitions of supramolecular polymer gel **6** (5.0 wt %) triggered by the change of temperature. (b) Optical images showing star supramolecular polymer **6** hydrogel samples in swollen state at 20 °C (<LCST) and in shrunken states at 50 °C (>LCST) in pure water. (c) The mechanism of thermosensitivity of supramolecular polymeric hydrogel. (d) Photographs of disassembly and reassembly of supramolecular polymeric hydrogel. (e) The mechanism of disassembly of supramolecular polymeric hydrogel induced by bromide anion.

was swollen and absorbed a significant amount of water. When the temperature was increased over LCST, the hydrogel was found to release free water and began to shrink (Figure 7c). For example, as shown in Figure 7b, the photographs of hydrogel **6** with a calibrated scale were recorded. A dramatic diameter decrease was observed with the increase of temperature. The diameter-change trend of the hydrogel **6** as a function of temperature was expressed by the diameter ratio in Figure S7. It was found that the hydrogel did not show obvious change below 25 °C. However, the hydrogel shrank very quickly up to 25 °C. Finally, the diameter of the hydrogel decreased from 2.0 to 0.8 cm at 45 °C, shrinking to 40%. This test showed the thermoresponsive phase transition behavior and a sharp decrease happened around the LCST. Critical transition temperatures for volume phase-transition were determined to be 25 °C via the tube inverting approach during the heating process.

It is well-known that the gel-phase transition can be determined from dynamic rheological data. The temperature at which the elastic modulus G' curve intersects that of the viscous modulus G'' usually indicates the gel-phase transition. Thus, besides the frequency sweep, oscillatory temperature ramp experiment was performed from 20 to 35 °C at a heating rate of 1.0 K/min with a fixed stress of 1.0 Pa and frequency of 1.0 rad/s. When the temperature was below 25 °C, both G' and G'' were quite low, while the G' was always much larger than G'', confirming a gel state. When the temperature was increased above 25 °C, both G' and G'' increased dramatically, and G'' increased faster than G'. A G'/G'' crossover point was observed around 29 °C, which was related to the phase transition of PNIPAAM hydrogel (Figure 6b). Because the hydrogel displayed a volume phase-transition rather than a sol−gel transition upon increasing the temperature, the G' and G'' showed an irregular change above this point, indicating the collapse of hydrogel. These observed phenomena further confirmed the thermo-response of the resultant polymeric hydrogels.

Inspired by the applications of dynamic characteristics of coordination metal−ligand bonds in the area of multicomponent self-organization and supramolecular transformations,[22] the reversible stimuli-responsive gel−sol transition of the resultant polymer hydrogels was expected because this family of cross-linked polymer gel was derived from the functionalized metallacycles. Bromide ion (Br⁻), as an effective stimulus to induce the disassembly of coordination-driven self-assembled metallacycles, was adopted in this study. As expected, it was found that the addition and removal of bromide ion (Br⁻) led to the reversible gel−sol transitions. As shown in Figure 7d, the polymeric hydrogel **6** gradually collapsed and ultimately became a turbid solution with the addition of tetrabutylammonium bromide (Bu₄NBr), and the reformation of the gel was achieved upon treatment of the turbid solution with a slight excess of silver hexafluorophosphate (AgOTf). As detected by SEM measurement (Figures S9−S12), the regular porous networks of xerogel were also destroyed and turned into an irregular microstructure after the addition of Bu₄NBr. The in situ multinuclear NMR (¹H and ³¹P) investigation of **6** (Schemes S7 and S8) evidenced that this stimuli-responsive gel−sol phase transition was essentially a consequence of the halide-induced disassembly and reassembly of the hexagonal metallacycles (Figure 7e). The typical proton signals of the hexagonal metallacycle disappeared in the ¹H NMR spectrum along with an increase in coupling of flanking ¹⁹⁵Pt satellites (ca. $\Delta J_{P-Pt} = 66$ Hz) in the ³¹P NMR spectrum upon addition of Bu₄NBr, indicating the complete disassembly of the hexagonal metallacycle. The original signals in the ¹H and ³¹P NMR spectra were restored after the addition of AgOTf to the mixture, demonstrating the quantitative reassembly of the supramolecular hexagonal metallacycles (Figure S13). A similar stimuli-responsive gel−sol transition induced by Br⁻ was observed for polymeric hydrogel **7** by taking advantage of the dynamic nature of Pt−N bonds (Figure S14).

Because the obtained hydrogels possessed chemical stimuli-responsibility, it was rationally expected that they could be

employed to encapsulate and release small molecules. Sulforhodamine B (SRB), as a fluorescent dye, was selected as a model for encapsulation and release investigation. First, the SRB was added into an aqueous solution of the star supramolecular polymer **6** (5.0 wt %), and the SRB-encapsulated hydrogel was formed from the mixed solution after a few minutes. Additionally, the amount of released of SRB was analyzed by UV absorbance of the solution at 562 nm (Figure S18). Figure 8 showed the release curve of SRB with
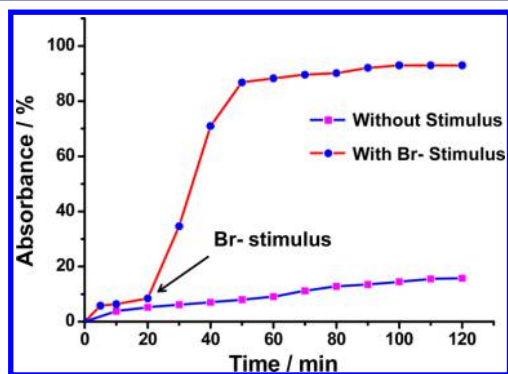

Figure 8. Release profile of SRB from star supramolecular hydrogel **6**. The red line represents the profile obtained in the presence of Bu$_4$NBr stimulus, while the blue line represents the profile obtained without any stimulus at 25 °C.

and without external stimuli. It was found that the SRB was released very slowly without the external stimulus. Only 18% SRB was released from the hydrogel even after 120 min. However, with the existence of Bu$_4$NBr, the SRB was released very quickly from the hydrogel due to the collapse of hydrogels induced by Br$^-$. The cumulative amount of SRB released from the hydrogel quickly reached about 90% after 50 min. Thus, these cross-linked supramolecular polymer hydrogels can be employed to encapsulate and release functional molecules over a tunable time and quantity through the artificial control.

Macroscopic Self-Healing Property of Supramolecular Polymeric Hydrogels. To obtain the further insight into the property of the resultant stimuli-responsive hydrogels, the additional rheological investigation of hydrogel **6** (5.0 wt %) was investigated under small (0.1%) and large (5000%) strains, respectively. Under the small (0.1%) strain, G' was found to be larger than G'', indicating the existence of the free-standing hydrogel. However, under the large (5000%) strain, G'' was larger than G', instead inferring the conversion from gel to sol state. Unexpectedly, as shown in Figure 9, the G' and G'' of the hydrogel **6** were approximate fully recovered in a half minute even under 5000% strain, and the recovery behavior was repeatable for at least four cycles of different strains. This finding indicated that the resultant polymeric hydrogel might feature a self-healing property.[23]

Inspired by the above rheological data, the self-healing property of the resultant polymeric hydrogel was studied. Cut-and-heal tests were conducted with the supramolecular hydrogel **6**. As depicted in Figure 10 and video 1, two disks of hydrogels were prepared, of which one hydrogel disk was colored with a SRB dye to render a better contrast, and the other is colorless. These two disks of hydrogel then were cut into two halves, and placed together at room temperature. Surprisingly, after only 1 min, the two pieces rejoined into one piece, and the crack at the damage site disappeared. The healed
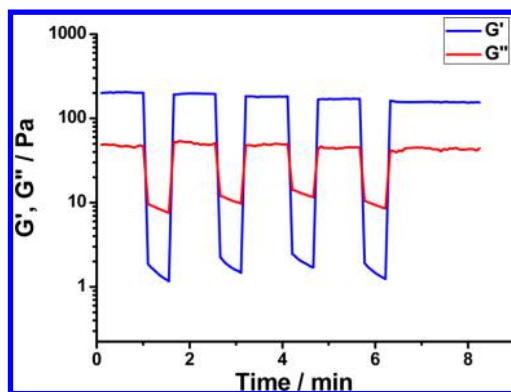

Figure 9. Continuous step strain measurements. 3.0 wt % hydrogel of star supramolecular polymer **6** was subject to 5000% strain for 30 s, then back to 0.1% strain in the linear regime for 60 s. This process was repeated for four cycles. Measurements were taken at 20 °C with a fixed frequency of 5.0 rad/s.

hydrogel could be lifted against its own weight. After 24 h, it was found that the color pink gradually spread into the colorless part, which again verified the self-healing behavior. Both the shape and the rheological properties (Figure S19) convinced that the hydrogels were recovered into the initial state.

We assumed that the macroscopic self-healing of supramolecular polymeric hydrogels was mainly caused by the dynamic nature of metallacycles. When the halves of gels were placed together, the dynamic assembly/disassembly of metallacycles allowed for the self-healing of hydrogels as displayed in Figure 10b. To obtain further evidence for such hypothesis, the self-healing behavior of the polymeric hydrogels with the existence of bromide ions (Br$^-$) stimulus was investigated as well. A hydrogel of **6** (5.0 wt %) was cut in half and coated with the aqueous solution of tetrabutylammonium bromide (Bu$_4$NBr) (2 mg/mL) being spread onto the cut surfaces. These two pieces then were put together. Different from the previous self-healing test without Br$^-$, the self-healing phenomenon was not observed even after 5 min (Figure 11). This finding supported that the driving force of self-healing behavior was mainly attributed to the metal–ligand coordination interactions within metallacycles.

■ CONCLUSION

In summary, we have demonstrated that the combination of coordination-driven self-assembly and postassembly polymerization allowed for the construction of a new family of supramolecular star polymers with stimuli-responsive properties. In this study, hexagonal metallacycles decorated with three CTAs at alternative vertexes were obtained from a newly designed 120° dipyridyl building block **1** and the corresponding complementary 120° di-Pt(II) acceptors **2** or **3** via coordination-driven self-assembly. The preparation is straightforward and in nearly quantitative yield, thus eliminating the need of purification. The tris-CTAs metallacycles were then employed as RAFT agent to prepare supramolecular star polymers through the controlled radical polymerization of N-isopropylacrylamide (NIPAAM). As expected, the resultant star polymers displayed lower critical solution temperature (LCST) behavior in water because of the introduction of PNIPAAM moieties onto the metallacycles. Interestingly, supramolecular polymer hydrogels cross-linked by discrete
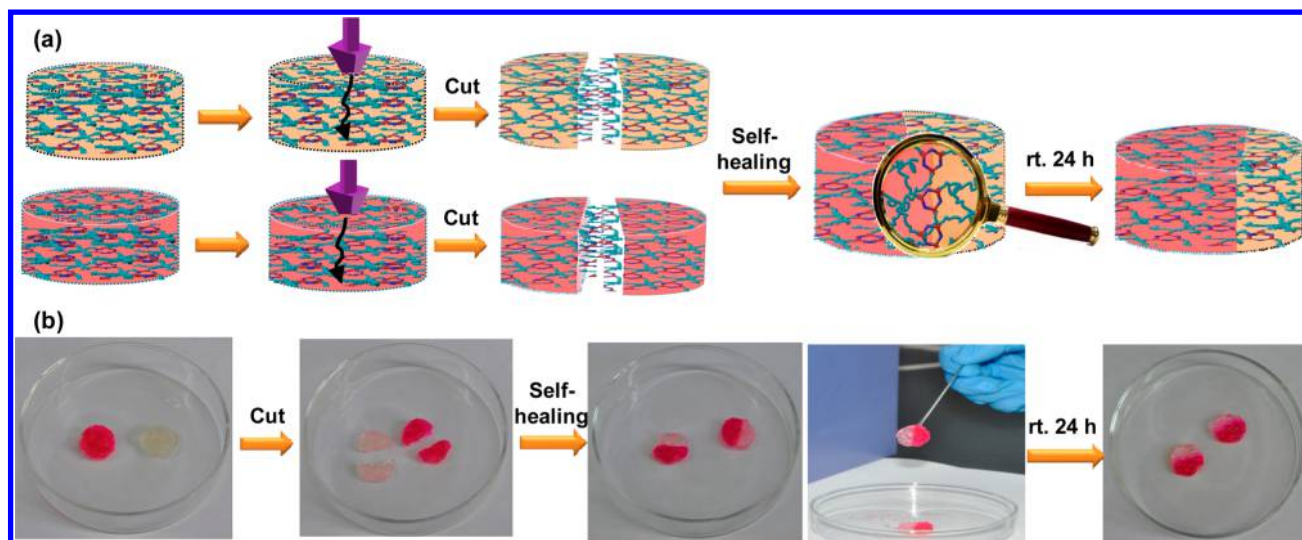
Figure 10. Rapid macroscopic self-healing experiments of the supramolecular polymeric hydrogel. (a) The mechanism of self-healing of the supramolecular polymeric hydrogel. (b) Photographs of the self-healing experiments.
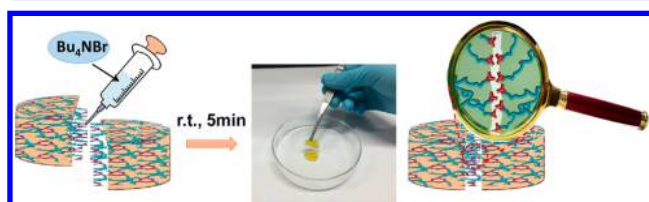

Figure 11. Br^--responsive self-healing test of the star polymer **6** hydrogel in the presence of Bu_4NBr. A hydrogel (5.0 wt %) was cut in half, and then Bu_4NBr aq was spread on the cut surface. Self-healing was not observed even after 5 min.

metallacycles were obtained from the star polymers at room temperature without heating–cooling process. Different from the most known PNIPAAM hydrogels, besides the thermoresponsive behavior, the existence of metallacyclic scaffold endowed the obtained polymeric hydrogels bromide anion stimuli-responsive and self-healing properties by taking advantage of the dynamic nature of Pt–N bonds in the hexagonal metallacycles.

It should be noted that the development of supramolecular gels cross-linked by discrete metallosupramolecular structures has received increasing attention very recently.[24] It is believed that the existence of a discrete metal–organic assembly gives rise to the preparation of novel smart soft matters because of the dynamic nature of metal–ligand bonds as well as the well-defined organometallic scaffold in gels. In this study, we successfully extended the scope of the postassembly modification strategy from the simple structure conversion through the easy covalent reactions to the controlled radical polymerization. By employing the new strategy, a new family of polymeric hydrogels cross-linked by well-defined, discrete metallacycles was realized, which featured interesting stimuli-responsive and self-healing behaviors. Thus, this study opened a new avenue to the construction of novel functional materials based on well-defined metallosupramolecular assemblies, in particular "smart" soft matters.

■ EXPERIMENTAL SECTION

Full experimental details are provided in the Supporting Information. The most important information is summarized briefly.

General Information. All reagents were commercially available and used as received unless stated otherwise. *N*-Isopropylacrylamide (NIPAAM was recrystallized twice from hexane prior to use) and azodiisobutyronitrile (AIBN was recrystallized from ethanol before use) were purchased from Energy Chemical Reagent Co. 2-Methyl-2-[(dodecylsulfanylthiocarbony) sulfanyl] propanic acid was purchased from J&K Co. TLC analyses were performed on silica-gel plates, and flash chromatography was conducted using silica-gel column packages. All solvents were dried according to standard procedures, and all of them were degassed under N_2 for 30 min before use. All air-sensitive reactions were carried out under argon atmosphere. ^{1}H NMR, ^{13}C NMR, and ^{31}P NMR spectra were recorded on a Bruker 400 MHz spectrometer (^{1}H, 400 MHz; ^{13}C, 100 MHz; ^{31}P, 161.9 MHz) and a Bruker 500 MHz spectrometer (^{1}H, 500 MHz) at 298 K. The ^{1}H and ^{13}C NMR chemical shifts are reported relative to residual solvent signals, and ^{31}P NMR resonances are referenced to internal standard sample of 85% H_3PO_4 (δ 0.0). Coupling constants (J) are denoted in Hz, and chemical shifts (δ) are in ppm. Multiplicities are denoted as follows: s = singlet, d = doublet, m = multiplet, br = broad. IR spectra were recorded on a Bruker Tensor 27 infrared spectrophotometer.

Transmission Electron Microscopy (TEM) and Dynamic Light Scattering (DLS) Studies. TEM images were recorded on a Tecnai G^2 F30 (FEI Ltd.). The sample for TEM measurements was prepared by dropping the solution onto a carbon-coated copper grid. The TEM sample of aggregates at the temperature above the LCST was prepared by spreading a droplet of the diluted solutions that had been preheated to a certain temperature (40 °C) onto a hot copper grid covered with carbon film at the same temperature, and drying in air under vacuum overnight at 40 °C. DLS measurements were performed under LV/5000E laser light scattering (LLS) spectrometers at a scattering angle of 90° and a temperature of 20–45 °C. CONTIN analysis was used for the extraction of Rh data.

Scanning Electron Microscopy (SEM) and Atomic Force Microscopy (AFM) Experiments. The SEM samples were prepared on clean Si substrates. To minimize sample charging, a thin layer of Au was deposited onto the samples before SEM examination. All of the SEM images were obtained using S-4800 (Hitachi Ltd.) with an accelerating voltage of 3.0–10.0 kV. AFM images were obtained on a Dimension FastScan (Bruker), using ScanAsyst mode under ambient condition. Scanasyst-Fluid$^+$ probes were used for the scan, and samples were prepared by dropping solutions onto a silicon wafer.

Gel Permeation Chromatography (GPC) Protocols. Gel permeation chromatography (GPC) analysis was carried out with a Waters Breeze 1515 GPC analysis system with TOSOH TSK gel α-3000 and α-2500 columns in series, using DMF with 0.5 M LiBr as

eluents at the flow rate of 1 mL/min at 80 °C. PEG calibration kit (purchased from TOSOH) was used as the calibration standard.

UV−Vis Absorption Spectra. UV−vis spectra were recorded in a quartz cell (light path 10 mm) on a Cary 50 Bio UV−vis spectrophotometer. UV−vis spectra were recorded in a conventional quartz cell (light path 10 mm) on a UV-2550 spectrophotometer from Shimadzu, Japan.

Dynamic Rheology Measurements. Rheological measurements were carried out on freshly prepared gels using a controlled stress rheometer (HAAKE MARSIII, Thermo Fisher). A parallel plate geometry of 25 mm diameter and a 0.3 mm gap were employed throughout dynamic oscillatory work. The following tests were performed: increasing amplitude of oscillation up to 100% apparent strain shear (kept a frequency of 1 rad s^{-1}) and frequency sweeps at 20 °C (from 50−0.1 rad s^{-1}).

Synthesis of 4. The dipyridyl donor ligand **1** (20.28 mg, 31.54 μmol) and the organoplatinum 120° acceptor **2** (44.41 mg, 33.11 μmol) were weighed accurately into a glass vial. To the vial was added 5.0 mL of acetone, and the reaction solution was then stirred at room temperature for 8 h to yield a homogeneous yellow solution. Yellow solid product **4** was obtained by removing the solvent under vacuum. Yield: 64.68 mg, >95%. Mp: >285 °C, decomposed. ^{1}H NMR (acetone-d_6, 400 MHz): δ 9.11−9.12 (d, 4H, J = 5.1 Hz), 7.97−7.99 (d, 4H, J = 5.6 Hz), 7.91 (s, 1H), 7.69−7.71 (d, 4H, J = 7.88 Hz), 7.57−7.58 (d, 6H, J = 6.52 Hz), 3.42−3.45 (t, 3H, J = 7.12), 1.88 (s, 2H), 1.72−1.78 (m, 2H), 1.49−1.50 (d, 14H, J = 3.4 Hz), 1.16−1.26 (m, 22H), 0.84−0.88 (t, 2H, J = 6.46 Hz). ^{31}P NMR (acetone-d_6, 161.9 MHz): δ 14.50 (s, $J_{Pt−P}$ = 2652.4 Hz). IR (neat): 2965, 2926, 2217, 2118, 1757, 1609, 1576, 1416, 1258, 762 cm^{-1}. ESI-TOF-MS of **4**: calcd for $[M − 5OTf]^{5+}$, 1040.54; found, 1040.60; calcd for $[M − 4OTf]^{4+}$, 1337.92; found, 1337.84.

Synthesis of 5. The dipyridyl donor ligand **1** (11.47 mg, 17.84 μmol) and the organoplatinum 120° acceptor **3** (28.71 mg, 21.04 μmol) were weighed accurately into a glass vial. To the vial were added 2.0 mL of acetone and 2.0 mL of DCM, and the reaction solution was then stirred at room temperature for 8 h to yield a homogeneous yellow solution. Yellow solid product **5** was obtained by removing the solvent under vacuum. Yield: 40.08 mg, >95%. Mp: >285 °C, decomposed. ^{1}H NMR (CD$_2$Cl$_2$, 400 MHz): δ 8.64 (s, 4H), 7.87−7.90 (d, 5H, J = 11.2 Hz), 7.91 (s, 1H), 7.47 (s, 2H), 7.24 (s, 2H), 7.06 (s, 1H), 3.36 (s, 2H), 1.80−1.86 (br, 15H), 1.64 (s, 10H, J = 3.4 Hz), 1..25 (br, 12H), 0.88 (s, 5H). ^{31}P NMR (CD$_2$Cl$_2$, 161.9 MHz): δ 16.35 (s, $J_{Pt−P}$ = 2296.4 Hz). IR (neat): 2963, 2925, 2216, 1754, 1574, 1260, 1145, 759 cm^{-1}. ESI-TOF-MS of **5**: calcd for $[M − 5OTf]^{5+}$, 1053.67; found, 1053.65; calcd for $[M − 4OTf]^{4+}$, 1354.33; found, 1354.45.

Synthesis of 6. Supramolecular [3+3] hexagons **4** (40 mg, 6.72 μmol), AIBN (0.5 mg, 3.36 μmol), *N*-isopropylacrylamide (450 mg, 4.0 mmol), and 1.0 mL of acetone were added to a 10 mL flask equipped with a magnetic stirring bar. After being degassed by freeze−pump−thaw cycles three times, the mixed solution was immediately transferred to a preheated 60 °C oil bath to initiate the polymerization. After 4 h, the polymerization was quenched by liquid N$_2$, and the resulting mixture was precipitated in diethyl ether. The precipitate was dissolved in acetone and then precipitated again into an excess of diethyl ether. The above dissolution−precipitation cycle was repeated three times. The final product was dried in a vacuum, yielding a yellow solid (225 mg, 50%, $M_{n,NMR}$ = 52 000 g/mol, $M_{n,GPC}$ = 43 000 g/mol, PDI = 1.25). ^{1}H NMR (acetone-d_6, 400 MHz): 6.80−7.45 (br s, −N*H*), 4.00 (br s, −NC*H*), 1.1−2.06 (br m, backbone), 0.84−0.88 (s, −C*H*$_3$ end-group). ^{31}P NMR (acetone-d_6, 161.9 MHz): δ 14.45 (s, $J_{Pt−P}$ = 2660 Hz). IR (neat): 3291, 2971, 2932, 2876, 1650, 1538, 1459, 1171 cm^{-1}.

Synthesis of 7. Supramolecular [3+3] hexagons **5** (40 mg, 6.6 μmol), AIBN (0.54 mg, 3.36 μmol), *N*-isopropylacrylamide (450 mg, 4 mmol), and 1.0 mL of acetone were added to a 10 mL flask equipped with a magnetic stirring bar. After being degassed by freeze−pump−thaw cycles three times, the mixed solution was immediately transferred to a preheated 60 °C oil bath to initiate the polymerization. After 4 h, the polymerization was quenched by liquid N$_2$, and the

resulting mixture was precipitated in diethyl ether. The precipitate was dissolved in acetone and then precipitated again into an excess of diethyl ether. The above dissolution precipitation cycle was repeated three times. The final product was dried in a vacuum, yielding a yellow solid (330 mg, 55%, $M_{n,NMR}$ = 63 000 g/mol, $M_{n,GPC}$ = 57 000 g/mol, PDI = 1.28). ^{1}H NMR (acetone-d_6, 400 MHz): 6.0−7.0 (br s, −N*H*), 4.00 (br s, −NC*H*), 1.1−2.06 (br m, backbone), 0.88 (s, −C*H*$_3$ end-group). ^{31}P NMR (acetone-d_6, 161.9 MHz): δ 16.32 (s, $J_{Pt−P}$ = 2298.9 Hz). IR (neat): 3292, 2972, 2934, 1740, 1541, 1457, 1370, 1223, 1056 cm^{-1}.

■ ASSOCIATED CONTENT

ⓈSupporting Information

The Supporting Information is available free of charge on the ACS Publications website at DOI: 10.1021/jacs.6b01089.

> Synthesis, characterization, and other experimental details (PDF)
> Video showing cut-and-heal test (AVI)

■ AUTHOR INFORMATION

Corresponding Authors
*guosong@fudan.edu.cn
*hbyang@chem.ecnu.edu.cn

Notes
The authors declare no competing financial interest.

■ ACKNOWLEDGMENTS

■ REFERENCES

(1) (a) Stang, P. J.; Olenyuk, B. *Acc. Chem. Res.* **1997**, *30*, 502. (b) Seidel, S. R.; Stang, P. J. *Acc. Chem. Res.* **2002**, *35*, 972. (c) Cook, T. R.; Zheng, Y.; Stang, P. J. *Chem. Rev.* **2013**, *113*, 734. (d) Chakrabarty, R.; Mukherjee, P. S.; Stang, P. J. *Chem. Rev.* **2011**, *111*, 6810. (e) Fujita, M.; Tominaga, M.; Hori, A.; Therrien, B. *Acc. Chem. Res.* **2005**, *38*, 369. (f) Nitschke, J. R. *Acc. Chem. Res.* **2007**, *40*, 103. (g) Castilla, A.; Ramsay, W.; Nitschke, J. R. *Acc. Chem. Res.* **2014**, *47*, 2063. (h) Pluth, M. D.; Raymond, K. N. *Chem. Soc. Rev.* **2007**, *36*, 161. (i) Oliveri, C. G.; Ulmann, P. A.; Wiester, M. J.; Mirkin, C. A. *Acc. Chem. Res.* **2008**, *41*, 1618. (j) Clever, A. H.; Shionoya, M. *Coord. Chem. Rev.* **2010**, *254*, 2391. (k) Takezawa, Y.; Shionoya, M. *Acc. Chem. Res.* **2012**, *45*, 2066. (l) Han, M.; Engelhard, D. M.; Clever, G. H. *Chem. Soc. Rev.* **2014**, *43*, 1848. (m) Han, Y.-F.; Jin, G.-X. *Acc. Chem. Res.* **2014**, *47*, 3571. (n) Liu, S.; Han, Y.-F.; Jin, G.-X. *Chem. Soc. Rev.* **2007**, *36*, 1543. (o) Yoshizawa, M.; Klosterman, J. K. *Chem. Soc. Rev.* **2014**, *43*, 1885. (p) Castilla, A. M.; Ramsay, W. J.; Nitschke, J. R. *Chem. Lett.* **2014**, *43*, 256.

(2) (a) Fujita, M.; Yazaki, J.; Ogura, K. *J. Am. Chem. Soc.* **1990**, *112*, 5645. (b) Fujita, M.; Oguro, D.; Miyazawa, M.; Oka, H.; Yamaguchi, K.; Ogura, K. *Nature* **1995**, *378*, 469. (c) Stang, P. J.; Cao, D. H. *J. Am. Chem. Soc.* **1994**, *116*, 4981. (d) Olenyuk, B.; Whiteford, J. A.; Fechtenkötter, A.; Stang, P. J. *Nature* **1999**, *398*, 796. (e) Lee, S. J.; Lin, W. *J. Am. Chem. Soc.* **2002**, *124*, 4554. (f) Brown, A. M.; Ovchinnikov, M. V.; Stern, C. L.; Mirkin, C. A. *J. Am. Chem. Soc.* **2004**, *126*, 14316. (g) Wang, P.; Moorefield, C. N.; Newkome, G. R. *Angew. Chem., Int. Ed.* **2005**, *44*, 1679. (h) Dong, V. M.; Fiedler, D.; Carl, B.; Bergman, R. G.; Raymond, K. N. *J. Am. Chem. Soc.* **2006**, *128*, 14464. (i) Harano, K.; Hiraoka, S.; Shionoya, M. *J. Am. Chem. Soc.* **2007**, *129*,

5300. (j) Bar, A. K.; Chakrabarty, R.; Mostafa, G.; Mukherjee, P. S. *Angew. Chem., Int. Ed.* **2008**, *47*, 8455. (k) Meng, W.; Clegg, J. K.; Thoburn, J. D.; Nitschke, J. R. *J. Am. Chem. Soc.* **2011**, *133*, 13652. (l) Wood, C. S.; Ronson, T. K.; Belenguer, A. M.; Holstein, J. J.; Nitschke, J. R. *Nat. Chem.* **2015**, *7*, 354. (m) Clever, G. H.; Kawamura, W.; Tashiro, S.; Shiro, M.; Shionoya, M. *Angew. Chem., Int. Ed.* **2012**, *51*, 2606. (n) Wang, M.; Wang, C.; Hao, X.-Q.; Li, X.; Vaughn, T. J.; Zhang, Y.-Y.; Yu, Y.; Li, Z.-Y.; Song, M.-P.; Yang, H.-B.; Li, X. *J. Am. Chem. Soc.* **2014**, *136*, 10499. (o) Sun, B.; Wang, M.; Lou, Z.; Huang, M.; Xu, C.; Li, X.; Chen, L.-J.; Yu, Y.; Davis, G. L.; Xu, B.; Yang, H.-B.; Li, X. *J. Am. Chem. Soc.* **2015**, *137*, 1556. (p) Whang, D.; Kim, K. *J. Am. Chem. Soc.* **1997**, *119*, 451. (q) Whang, D.; Park, K.-M.; Heo, J.; Ashton, P.; Kim, K. *J. Am. Chem. Soc.* **1998**, *120*, 4899. (r) Kishi, N.; Akita, M.; Kamiya, M.; Hayashi, S.; Hsu, H.-F.; Yoshizawa, M. *J. Am. Chem. Soc.* **2013**, *135*, 12976. (s) Kishi, N.; Li, Z.; Yoza, K.; Akita, M.; Yoshizawa, M. *J. Am. Chem. Soc.* **2011**, *133*, 11438.

(3) (a) Cook, T. R.; Vajpayee, V.; Lee, M. H.; Stang, P. J.; Chi, K. *Acc. Chem. Res.* **2013**, *46*, 2464. (b) Pluth, M. D.; Bergman, R. G.; Raymond, K. N. *Acc. Chem. Res.* **2009**, *42*, 1650. (c) Zhao, C.; Sun, Q.; Hart-Cooper, W. M.; Dipasquale, A. G.; Toste, F. D.; Bergman, R. G.; Raymond, K. N. *J. Am. Chem. Soc.* **2013**, *135*, 18802. (d) Mondal, B.; Acharyya, K.; Howlader, P.; Mukherjee, P. S. *J. Am. Chem. Soc.* **2016**, *138*, 1709. (e) Howlader, P.; Das, P.; Zangrando, E. *J. Am. Chem. Soc.* **2016**, *138*, 1668. (f) Roy, B.; Ghosh, A. K.; Srivastava, S.; Mukherjee, P. S. *J. Am. Chem. Soc.* **2015**, *137*, 11916. (g) Chen, L.-J.; Ren, Y.-Y.; Wu, N.-W.; Sun, B.; Ma, J.-Q.; Tan, H.; Liu, M.; Li, X.; Yang, H.-B. *J. Am. Chem. Soc.* **2015**, *137*, 11725. (h) Jiang, B.; Zhang, J.; Ma, J.-Q.; Zheng, W.; Chen, L.-J.; Sun, B.; Li, C.; Hu, B.-W.; Tan, H.; Li, X.; Yang, H.-B. *J. Am. Chem. Soc.* **2016**, *138*, 738. (i) Xuan, W.; Zhang, M.; Liu, Y.; Chen, Z.; Cui, Y. *J. Am. Chem. Soc.* **2012**, *134*, 6904. (j) Omagari, T.; Suzuki, A.; Akita, M.; Yoshizawa, M. *J. Am. Chem. Soc.* **2016**, *138*, 499. (k) Aliprandi, A.; Genovese, D.; Mauro, M.; Cola, L. D. *Chem. Lett.* **2015**, *44*, 1152.

(4) (a) Han, M.; Michel, R.; He, B.; Chen, Y.-S.; Stalke, D.; John, M.; Clever, G. H. *Angew. Chem., Int. Ed.* **2013**, *52*, 1319. (b) Freye, S.; Michel, R.; Stalke, D.; Pawliczek, M.; Frauendorf, H.; Clever, G. H. *J. Am. Chem. Soc.* **2013**, *135*, 8476. (c) Zhu, R.; Lübben, J.; Dittrich, B.; Clever, G. H. *Angew. Chem., Int. Ed.* **2015**, *54*, 2796. (d) Hiraoka, S.; Harano, K.; Shiro, M.; Shionoya, M. *J. Am. Chem. Soc.* **2008**, *130*, 14368. (e) Bhat, I. A.; Samanta, D.; Mukherjee, P. S. *J. Am. Chem. Soc.* **2015**, *137*, 9497. (f) Samanta, D.; Mukherjee, P. S. *J. Am. Chem. Soc.* **2014**, *136*, 17006. (g) Mukherjee, S.; Mukherjee, P. S. *Chem. Commun.* **2014**, *50*, 2239. (h) Shanmugaraju, S.; Mukherjee, P. S. *Chem. - Eur. J.* **2015**, *21*, 6656. (i) Smulders, M. M. J.; Jiménez, A.; Nitschke, J. R. *Angew. Chem., Int. Ed.* **2012**, *51*, 6681. (j) Sarma, R. J.; Nitschke, J. R. *Angew. Chem., Int. Ed.* **2008**, *47*, 377. (k) Yamashina, M.; Sartin, M. M.; Sei, Y.; Akita, M.; Takeuchi, S.; Tahara, T.; Yoshizawa, M. *J. Am. Chem. Soc.* **2015**, *137*, 9266. (l) Okazawa, Y.; Kondo, K.; Akita, M.; Yoshizawa, M. *J. Am. Chem. Soc.* **2015**, *137*, 98. (m) Xu, L.; Chen, L.-J.; Yang, H.-B. *Chem. Commun.* **2014**, *50*, 5156. (n) Xu, L.; Wang, Y.-X.; Yang, H.-B. *Dalton Trans.* **2015**, *44*, 867. (o) Xu, L.; Wang, Y.-X.; Chen, L.-J.; Yang, H.-B. *Chem. Soc. Rev.* **2015**, *44*, 2148. (p) McConnell, A. J.; Wood, C. S.; Neelakandan, P. P.; Nitschke, J. R. *Chem. Rev.* **2015**, *115*, 7729.

(5) (a) Wei, P.; Cook, T. R.; Yan, X.; Huang, F.; Stang, P. J. *J. Am. Chem. Soc.* **2014**, *136*, 15497. (b) Yan, X.; Li, S.; Cook, T. R.; Ji, X.; Yao, Y.; Pollock, J. B.; Shi, Y.; Yu, G.; Li, J.; Huang, F.; Stang, P. J. *J. Am. Chem. Soc.* **2013**, *135*, 14036. (c) Yan, X.; Jiang, B.; Cook, T. R.; Zhang, Y.; Li, J.; Yu, Y.; Huang, F.; Yang, H.-B.; Stang, P. J. *J. Am. Chem. Soc.* **2013**, *135*, 16813. (d) Yan, X.; Li, S.; Pollock, J. B.; Cook, T. R.; Chen, J.; Zhan, Y.; Ji, X.; Yu, Y.; Huang, F.; Stang, P. J. *Proc. Natl. Acad. Sci. U. S. A.* **2013**, *110*, 15585.

(6) (a) Dawson, P. E.; Muir, T. W.; Clark-Lewis, I.; Kent, S. B. *Science* **1994**, *266*, 776. (b) Blanco-Canosa, J. B.; Dawson, P. E. *Angew. Chem., Int. Ed.* **2008**, *47*, 6851. (c) Franke, R.; Doll, C.; Eichler, J. *Tetrahedron Lett.* **2005**, *46*, 4479. (d) Khan, S.; Sur, S.; Dankers, P.; Stupp, S. I. *Bioconjugate Chem.* **2014**, *25*, 707. (e) Hang, H. C.; Bertozzi, C. R. *Bioorg. Med. Chem.* **2005**, *13*, 5021. (f) Yang, X.-J. *Oncogene* **2005**, *24*,

1653. (g) Yang, X.-J.; Seto, E. *Mol. Cell* **2008**, *31*, 449. (h) Agard, N. J.; Bertozzi, C. R. *Acc. Chem. Res.* **2009**, *42*, 788.

(7) (a) Tanabe, K. K.; Cohen, S. M. *Chem. Soc. Rev.* **2011**, *40*, 498. (b) Wang, Z.; Cohen, S. M. *Chem. Soc. Rev.* **2009**, *38*, 1315. (c) Deng, H.; Doonan, C. J.; Furukawa, H.; Ferreira, R. B.; Towne, J.; Knobler, C. B.; Wang, B.; Yaghi, O. M. *Science* **2010**, *327*, 846. (d) Hoskins, B. F.; Robson, R. *J. Am. Chem. Soc.* **1990**, *112*, 1546. (e) Wang, Z.; Cohen, S. M. *J. Am. Chem. Soc.* **2007**, *129*, 12368. (f) Banerjee, M.; Das, S.; Yoon, M.; Choi, H. J.; Hyun, M. H.; Park, S. M.; Seo, G.; Kim, K. *J. Am. Chem. Soc.* **2009**, *131*, 7524.

(8) (a) Fuller, A.-M.; Leigh, D. A.; Lusby, P. J.; Oswald, I. D. H.; Parsons, S.; Walker, D. B. *Angew. Chem., Int. Ed.* **2004**, *43*, 3914. (b) Leigh, D. A.; Lusby, P. J.; McBurney, R. T.; Morelli, A.; Slawin, A. M. Z.; Thomson, A. R.; Walker, D. B. *J. Am. Chem. Soc.* **2009**, *131*, 3762. (c) Barran, P. E.; Cole, H. L.; Goldup, S. M.; Leigh, D. A.; McGonigal, P. R.; Symes, M. D.; Wu, J.; Zengerle, M. *Angew. Chem., Int. Ed.* **2011**, *50*, 12280. (d) Fuller, A.-M. L.; Leigh, D. A.; Lusby, P. J.; Slawin, A. M. Z.; Walker, D. B. *J. Am. Chem. Soc.* **2005**, *127*, 12612. (e) Beves, J. E.; Blight, B. A.; Campbell, C. J.; Leigh, D. A.; McBurney, R. T. *Angew. Chem., Int. Ed.* **2011**, *50*, 9260. (f) Dietrich-Buchecker, C. O.; Sauvage, J.-P.; Kern, J.-M. *J. Am. Chem. Soc.* **1984**, *106*, 3043. (g) Dietrich-Buchecker, C. O.; Sauvage, J.-P.; Kintzinger, J.-P. *Tetrahedron Lett.* **1983**, *24*, 5095. (h) Niess, F.; Duplan, V.; Sauvage, J.-P. *Chem. Lett.* **2014**, *43*, 964.

(9) (a) Barker, I. A.; Hall, D. J.; Hansell, C. F.; Du Prez, F. E.; O'Reilly, R. K.; Dove, A. P. *Macromol. Rapid Commun.* **2011**, *32*, 1362. (b) Konkolewicz, D.; Gray-Weale, A.; Perrier, S. *J. Am. Chem. Soc.* **2009**, *131*, 18075. (c) Sun, M. H.; Bo, Z. S. *J. Polym. Sci., Part A: Polym. Chem.* **2007**, *45*, 111. (d) Gody, G.; Rossner, C.; Moraes, J.; Vana, P.; Maschmeyer, T.; Perrier, S. *J. Am. Chem. Soc.* **2012**, *134*, 12596. (e) Ariga, K.; Yamauchi, Y.; Rydzek, G.; Ji, Q.; Yonamine, Y.; Wu, K. C.-W.; Hill, J. P. *Chem. Lett.* **2014**, *43*, 36. (f) Wang, X.-Q.; Wang, W.; Wang, Y.-X.; Yang, H.-B. *Chem. Lett.* **2015**, *44*, 1040.

(10) (a) Roberts, D. A.; Castilla, A. M.; Ronson, T. K.; Nitschke, J. R. *J. Am. Chem. Soc.* **2014**, *136*, 8201. (b) Zheng, Y.-R.; Lan, W.-J.; Wang, M.; Cook, T. R.; Stang, P. J. *J. Am. Chem. Soc.* **2011**, *133*, 17045. (c) Sun, S.-S.; Anspach, J. A.; Lees, A. J. *Inorg. Chem.* **2002**, *41*, 1862. (d) Sun, S.-S.; Stern, C. L.; Nguyen, S.-B. T.; Hupp, J. T. *J. Am. Chem. Soc.* **2004**, *126*, 6314. (e) Heo, J.; Jeon, Y.-M.; Mirkin, C. A. *J. Am. Chem. Soc.* **2007**, *129*, 7712. (f) Zhao, L.; Northrop, B. H.; Stang, P. J. *J. Am. Chem. Soc.* **2008**, *130*, 11886. (g) Campbell, V. E.; de, H. X.; Delsuc, N.; Kauffmann, B.; Huc, I.; Nitschke, J. R. *Nat. Chem.* **2010**, *2*, 684. (h) Wang, M.; Lan, W.-J.; Zheng, Y.-R.; Cook, T. R.; White, H. S.; Stang, P. J. *J. Am. Chem. Soc.* **2011**, *133*, 10752.

(11) Chakrabary, R.; Stang, P. J. *J. Am. Chem. Soc.* **2012**, *134*, 14738.

(12) Roberts, D. A.; Pilgrim, B. S.; Cooper, J. D.; Ronson, T. K.; Zarra, S.; Nitschke, J. R. *J. Am. Chem. Soc.* **2015**, *137*, 10068.

(13) Chen, S.; Chen, L.-J.; Yang, H.-B.; Tian, H.; Zhu, W. *J. Am. Chem. Soc.* **2012**, *134*, 13596.

(14) (a) Zetterlund, P. B.; Kagawa, Y.; Okubo, M. *Chem. Rev.* **2008**, *108*, 3747. (b) Yamago, S. *Chem. Rev.* **2009**, *109*, 5051. (c) Rosen, B. M.; Percec, V. *Chem. Rev.* **2009**, *109*, 5069. (d) Braunecker, W.; Matyjaszewski, K. *Prog. Polym. Sci.* **2007**, *32*, 93.

(15) (a) Moad, G.; Mayadunne, R.; Rizzardo, E.; Skidmore, M.; Thang, S. H. *Macromol. Symp.* **2003**, *192*, 1. (b) Zheng, G.; Pan, C. *Polymer* **2005**, *46*, 2802. (c) Zheng, G.; Pan, C. *Macromolecules* **2006**, *39*, 95. (d) Iovu, M.; Matyjaszewski, K. *Macromolecules* **2003**, *36*, 9346. (e) Hong, C.; You, Y.; Pan, C. *J. Polym. Sci., Part A: Polym. Chem.* **2004**, *42*, 4873. (f) You, Y.; Hong, C.; Wang, W.; Lu, W.; Pan, C. *Macromolecules* **2004**, *37*, 9761. (g) Zheng, Q.; Pan, C. *Macromolecules* **2005**, *38*, 6841.

(16) (a) Xia, J.; Matyjaszewski, K. *Chem. Rev.* **2001**, *101*, 2921. (b) Tsarevsky, N. V.; Matyjaszewski, K. *Chem. Rev.* **2007**, *107*, 2270. (c) Xia, J.; Zhang, X.; Matyjaszewski, K. *Macromolecules* **1999**, *32*, 4482. (d) Zhang, X.; Xia, J.; Matyjaszewski, K. *Macromolecules* **2000**, *33*, 2340.

(17) (a) Abrol, S.; Kambouris, P. A.; Looney, M. G.; Solomon, D. H. *Macromol. Rapid Commun.* **1997**, *18*, 755. (b) Narumi, A.; Satoh, T.; Kaga, H.; Kakuchi, T. *Macromolecules* **2002**, *35*, 699. (c) Bosman, A.

W.; Vestberg, R.; Heumann, A.; Hawker, C. *J. Am. Chem. Soc.* **2001**, *123*, 6461.

(18) (a) Stang, P. J.; Persky, N. E.; Manna, J. *J. Am. Chem. Soc.* **1997**, *119*, 4777. (b) Yang, H.-B.; Ghosh, K.; Zhao, Y.; Northrop, B. H.; Lyndon, M. M.; Muddiman, D. C.; White, H. S.; Stang, P. J. *J. Am. Chem. Soc.* **2008**, *130*, 839. (c) Zhao, G.-Z.; Li, Q.-J.; Chen, L.-J.; Tan, H.; Wang, C.-H.; Wang, D.-X.; Yang, H.-B. *Organometallics* **2011**, *30*, 5141. (d) Chen, L.-J.; Li, Q.-J.; He, J.; Tan, H.; Abliz, Z.; Yang, H.-B. *J. Org. Chem.* **2012**, *77*, 1148. (e) Wu, N.-W.; Zhang, J.; Ciren, D.; Han, Q.; Chen, L.-J.; Xu, L.; Yang, H.-B. *Organometallics* **2013**, *32*, 2536. (f) Wu, N.-W.; Chen, L.-J.; Wang, C.; Ren, Y.-Y.; Li, X.; Xu, L.; Yang, H.-B. *Chem. Commun.* **2014**, *50*, 4231.

(19) (a) Schild, H. G.; Tirrell, D. A. *Macromolecules* **1992**, *25*, 4553. (b) Okajima, S.; Sakai, Y.; Yamaguchi, T. *Langmuir* **2005**, *21*, 4043. (c) Hu, T.; You, Y.; Pan, C.; Wu, C. *J. Phys. Chem. B* **2002**, *106*, 6659. (d) Bergbreiter, D. E.; Caraway, J. W. *J. Am. Chem. Soc.* **1996**, *118*, 6092. (e) Chiefari, J.; Chong, Y. K.; Ercole, F.; Krstina, J.; Jeffery, J. *Macromolecules* **1998**, *31*, 5559.

(20) (a) Zhao, X. *Soft Matter* **2014**, *10*, 672. (b) Xu, D.; Hawk, J.; Loveless, D. M.; Jeon, S. L.; Craig, S. L. *Macromolecules* **2010**, *43*, 3556. (c) Xu, D.; Liu, C. Y.; Craig, S. L. *Macromolecules* **2011**, *44*, 2343. (d) Xu, D.; Craig, S. L. *Macromolecules* **2011**, *44*, 5465.

(21) (a) Hvidt, S.; Jorgensen, E. B. *J. Phys. Chem.* **1994**, *98*, 12320. (b) Almgren, M.; Brown, W.; Hvidt, S. *Colloid Polym. Sci.* **1995**, *273*, 2.

(22) (a) Zhao, G.-Z.; Chen, L.-J.; Wang, W.; Zhang, J.; Yang, G.; Wang, D.; Yu, Y.; Yang, H.-B. *Chem. - Eur. J.* **2013**, *19*, 10094. (b) Chen, L.-J.; Zhao, G.-Z.; Jiang, B.; Sun, B.; Wang, M.; Xu, L.; He, J.; Abliz, Z.; Tan, H.; Li, X.; Yang, H.-B. *J. Am. Chem. Soc.* **2014**, *136*, 5993. (c) Li, Z.-Y.; Zhang, Y.-Y.; Zhang, C.-W.; Chen, L.-J.; Wang, C.; Tan, H.; Yu, Y.; Li, X.; Yang, H.-B. *J. Am. Chem. Soc.* **2014**, *136*, 8577. (d) Wang, X.-Q.; Wang, W.; Yin, G.-Q.; Wang, Y.-X.; Zhang, C.-W.; Shi, J.-M.; Yu, Y.; Yang, H.-B. *Chem. Commun.* **2015**, *50*, 4231. (e) Wang, W.; Sun, B.; Wang, X.-Q.; Ren, Y.-Y.; Chen, L.-J.; Ma, J.; Zhang, Y.; Li, X.; Yu, Y.; Tan, H.; Yang, H.-B. *Chem. - Eur. J.* **2015**, *21*, 6286. (f) Wang, W.; Zhang, Y.; Sun, B.; Chen, L.-J.; Xu, X.-D.; Wang, M.; Li, X.; Yu, Y.; Jiang, W.; Yang, H.-B. *Chem. Sci.* **2014**, *5*, 4554.

(23) (a) Harada, A.; Takashima, Y.; Nakahata, M. *Acc. Chem. Res.* **2014**, *47*, 2128. (b) Nakahata, M.; Takashima, Y.; Yamaguchi, H.; Harada, A. *Nat. Commun.* **2011**, *2*, 511. (c) Ma, X.; Tian, H. *Acc. Chem. Res.* **2014**, *47*, 1971. (d) Zhang, M.; Xu, D.; Yan, X.; Chen, J.; Dong, S.; Zheng, B.; Huang, F. *Angew. Chem., Int. Ed.* **2012**, *51*, 7011.

(24) (a) Foster, J. A.; Parker, R. M.; Belenguer, A. M.; Kishi, N.; Sutton, S.; Abell, C.; Nitschke, J. R. *J. Am. Chem. Soc.* **2015**, *137*, 9722. (b) Zhukhovitskiy, A. V.; Zhong, M.; Keeler, E. G.; Michaelis, V. K.; Sun, J. E. P.; Hore, M. J. A.; Pochan, D. J.; Griffin, R. G.; Willard, A. P.; Johnson, J. A. *Nat. Chem.* **2015**, *8*, 33. (c) Kawamoto, K.; Grindy, S. C.; Liu, J.; Holten-Andersen, N.; Johnson, J. *ACS Macro Lett.* **2015**, *4*, 458.